

Somatic Mutational Mechanisms Involved in Intestinal Tumor Formation in Min Mice¹

Alex R. Shoemaker,² Cindy Luongo,² Amy R. Moser,³ Laurence J. Marton, and William F. Dove⁴

McArdle Laboratory for Cancer Research [A. R. S., C. L., A. R. M., L. J. M., W. F. D.], Laboratory of Genetics [A. R. S., C. L., W. F. D.], and Department of Pathology and Laboratory of Medicine [L. J. M.], University of Wisconsin Medical School, Madison, Wisconsin 53706

ABSTRACT

We have demonstrated previously that intestinal tumor formation in B6 *Min/+* mice is always accompanied by loss of the wild-type adenomatous polyposis coli (*Apc*) allele and that intestinal tumor multiplicity in B6 *Min/+* mice can be significantly increased by treatment with a single dose of *N*-ethyl-*N*-nitrosourea (ENU). Here, we show that some tumors from ENU-treated *Min/+* mice can form without complete elimination of *Apc*⁺. At least 25% of these tumors acquired somatic *Apc* truncation mutations. Interestingly, some ENU-induced tumors demonstrated loss of the *Apc*⁺ allelic marker examined by the quantitative PCR assay used here. Using two methods of mutation detection, we identified no *Apc* mutations in at least 12% of the tumors from ENU-treated B6 *Min/+* mice. Finally, no H- or K-*ras*-activating mutations were detected in intestinal tumors from either untreated or ENU-treated *Min/+* mice. The majority of somatic human *APC* mutations in intestinal tumors lead to *APC* truncation. Our results demonstrate that somatic *Apc* truncation mutations also frequently occur in ENU-induced intestinal tumors in *Min* mice.

INTRODUCTION

Mutation of the *APC*⁵ tumor suppressor gene is clearly associated with human intestinal tumorigenesis (1–8). FAP, an inherited cancer syndrome in which affected individuals develop as many as several thousand intestinal adenomas, results from germ-line *APC* mutation (2, 3, 9). Somatic mutation of the remaining wild-type allele of *APC* has been shown to be a very early, possibly initiating, event in the formation of a majority of intestinal tumors in FAP (5, 6). Furthermore, somatic mutation of *APC* frequently occurs in tumor formation in cases of sporadic intestinal cancer (5–8), as well as in hereditary nonpolyposis colon cancer, a familial cancer syndrome resulting from germ-line mutations of genes involved in DNA mismatch repair (10–14).

The *APC* gene encodes a 2843-amino acid protein that contains several potentially important functional domains (2–4). These include an NH₂-terminal region involved in homodimerization (15, 16), a COOH-terminal region involved in microtubule association (17, 18), and two centrally located regions that bind β -catenin (19–21). Catenins modulate cell-cell adhesion functions, in part via interaction with cadherins (22, 23).

The vast majority (>95%) of both germ-line and somatic *APC* mutations result in premature truncation of the *APC* polypeptide (5–8, 24). Most of these mutations occur within the first 1500 codons of the gene (5–8, 24). Germ-line mutations in *APC* tend to be scattered throughout the first half of the gene, although there appear to be two

“hot spots” at codons 1061 and 1309 (5–6, 25). Approximately two-thirds of identified somatic mutations are located in a MCR between codons 1286 and 1513 (5–7). The high frequency of *APC* mutations in the MCR suggests that mutations in this region of the gene may be more efficient at inducing tumor formation than mutations elsewhere in the gene (4). This idea is supported by the fact that germ-line *APC* mutations in the MCR frequently result in more severe polyposis (4, 6, 26).

Mutational activation of the *ras* oncogene has also been implicated as an important event in human intestinal cancer (27, 28). In particular, mutation of K-*ras* seems to be correlated with the development of large, dysplastic adenomatous polyps in humans. It has been shown that more than 50% of dysplastic polyps larger than 1.0 cm in size contain K-*ras* mutations, whereas only 9% of adenomas less than 1.0 cm have *ras* mutations (28).

We have been investigating intestinal neoplasia in the *Min* (multiple intestinal neoplasia) mouse, a model for human intestinal cancer (29, 30). *Min* is a nonsense mutation at codon 850 of *Apc*, the mouse homolog of human *APC* (30). The mouse *Apc* and human *APC* coding sequences are 86 and 90% identical at the nucleotide and amino acid levels, respectively (30). On the sensitive C57BL/6J (B6) background, mice heterozygous for *Apc*^{*Min*} can develop more than 50 adenomas throughout the entire intestinal tract and rarely live beyond 150 days of age (29).

It has been demonstrated that spontaneously arising intestinal tumors in B6 *Min/+* mice lose the wild-type allele of *Apc*, most commonly by whole chromosome loss (31–33). The somatic mutational mechanism(s) involved in intestinal tumor formation in *Min/+* mice can be altered through the use of somatic mutagenesis and manipulation of the genetic background (33). Using a quantitative PCR assay that examines a 155-bp region surrounding the *Min* mutation, Luongo and Dove (33) found that a small number of intestinal tumors from (129/SvJ × B6)F₁*Min/+* and (*Mus musculus castaneus* (CAST) × B6)F₁*Min/+* mice retained at least this portion of the *Apc*⁺ allele. Similar results were obtained for intestinal tumors analyzed from γ -irradiated (AKR/J (AKR) × B6)F₁*Min/+* mice (33). It is presently unknown whether any of these tumors acquired more subtle *Apc* mutations.

The role of activated *ras* in *Min*-induced tumorigenesis is unclear. Crosses of B6 *Min/+* mice to transgenic mice expressing an activated human K-*ras* allele did not result in increased intestinal tumor multiplicity or rate of progression (34). In contrast to this result, D'Abaco *et al.* (35) reported that expression of an activated H-*ras* allele in SV40-immortalized *Min/+* intestinal epithelial cells can induce tumor formation in nude mice, apparently without loss of the remaining wild-type *Apc* allele.

In this report, we examine in more detail the somatic mutational events involved in intestinal tumor formation in *Min* mice. We demonstrated previously that somatic mutagenesis of B6 *Min/+* mice with the alkylating agent ENU leads to significant increases in intestinal tumor multiplicity (36). Here, we show that these ENU-induced tumors in *Min/+* mice can form without complete deletion of *Apc*⁺. These tumors have been examined for the presence of intragenic

Received 10/4/96; accepted 3/24/97.

The costs of publication of this article were defrayed in part by the payment of page charges. This article must therefore be hereby marked *advertisement* in accordance with 18 U.S.C. Section 1734 solely to indicate this fact.

¹ This work was supported by Grant CA50585 and Core Grant CA07175 from the National Cancer Institute.

² Present address: Bock Laboratories, University of Wisconsin, Madison, WI 53706.

³ Present address: Department of Human Oncology, University of Wisconsin Comprehensive Cancer Center, Madison, WI 53792.

⁴ To whom requests for reprints should be addressed, at McArdle Laboratory for Cancer Research, University of Wisconsin Medical School, 1400 University Avenue, Madison, WI 53706.

⁵ The abbreviations used are: *APC*, adenomatous polyposis coli; FAP, familial adenomatous polyposis; MCR, mutation cluster region; ENU, *N*-ethyl-*N*-nitrosourea; ORF, open reading frame; RT, reverse transcription; IVSP, *in vitro* synthesized protein.

somatic *Apc* mutations and for activating mutations of the *ras* proto-oncogene.

MATERIALS AND METHODS

Mice. All mice were bred at the McArdle Laboratory for Cancer Research. B6 and AKR mice were originally purchased from The Jackson Laboratory (Bar Harbor, ME). The B6-*Min* pedigree is maintained by crossing B6 *Apc*^{+/+}/*Apc*^{+/+} females with B6 *Apc*^{Min}/*Apc*^{+/+} (*Min*/+) males. All B6-*Min* mice used in these experiments were from the 24th to 32nd backcross generations to B6. (AKR × B6)_{F1}*Min*/+ mice were produced by mating AKR females with B6 *Min*/+ males. Animals were genotyped for the presence of the *Min* mutation by the PCR-based assay described previously (37). Somatic treatment of mice with ENU was performed as described previously (36, 38, 39). B6 *Min*/+ mice were given a single i.p. injection of ENU at 5–35 days of age and then sacrificed approximately 65 days after treatment. Untreated B6 *Min*/+ mice were sacrificed at an age that corresponded to the final age of the ENU-treated mice (*i.e.*, 70–100 days of age).

Tissue Sample Collection. Isolation and dissection of the intestinal tract were carried out as detailed previously (36). Intestinal tumors and regions of normal intestinal epithelium were collected from (AKR × B6)_{F1}*Min*/+ mice, fixed in formalin, embedded, and sectioned as described by Luongo *et al.* (31). Intestinal tumor and normal intestinal tissue samples were collected from ENU-treated and untreated B6 *Min*/+ mice by three distinct methods. One set of 134 tumors and 54 normal tissue samples collected from 30 *Min*/+ animals was fixed in formalin and processed as described for the F₁ mice. A second set of 90 tumors and 18 normal tissue samples was collected from 15 *Min*/+ mice. Tumor samples were dissected from the intestine to be as free of normal tissue as possible. Dissection tools were cleaned between samples by rinsing with bleach. Tumors and normal tissue samples were quickly frozen in OCT embedding compound (Miles Scientific, Naperville, IL) over liquid N₂ vapor. A final set of 75 tumors and 28 normal tissue samples was collected from 17 *Min*/+ mice. Tumors were dissected as described above. In this case, each tumor or normal tissue sample was cut in half with a new razor blade. Tissue pieces were then placed in separate tubes and immediately frozen in liquid N₂. One sample was used for isolation of DNA, and the corresponding sample was used for isolation of RNA.

Nucleic Acid Isolation. Formalin-fixed samples were sectioned at 10- μ m thickness, and every tenth section was stained with H&E for histological assessment. DNA was prepared from scraped tissue obtained from unstained sections, as described previously (31). Samples embedded in OCT were also sectioned at 10- μ m thickness, and every tenth section was stained with H&E. Intervening sections (approximately 30 per sample) were collected directly into an Eppendorf tube containing 500 μ l of a digestion buffer consisting of 500 μ g/ml proteinase K, 1% SDS, 500 mM Tris (pH 9.0), 20 mM EDTA, and 10 mM NaCl (40). Samples were homogenized by vortexing and were then incubated overnight at 55°C. The samples were then extracted with phenol-chloroform and precipitated with ethanol. The DNA was resuspended in a final volume of 20 μ l of water. DNA was prepared from freshly frozen samples by resuspending the tissue in 500 μ l of the digestion buffer described above. Samples were homogenized with a micropestle (Kontes, Vineland, NJ) and then further sheared by pulling the homogenate through 18 and 25 gauge needles. Samples were incubated overnight at 55°C, extracted with phenol-chloroform, precipitated, and finally resuspended in 25 μ l of water. RNA was prepared from freshly frozen samples by the acid-guanidinium-phenol-chloroform method, scaled down for use in Eppendorf tubes (41). Samples were homogenized in guanidinium buffer with micropestles and syringes as described for DNA preparation. RNA was resuspended in 25 μ l of diethyl pyrocarbonate-treated water.

***Apc* Allelic Loss Analyses.** The relative ratios of the *Apc*⁺ to *Apc*^{Min} alleles were determined by a quantitative PCR assay (31). This assay uses modified PCR primers that flank the *Apc* mutation. Amplification of the wild-type *Apc* allele results in a 155-bp PCR product with two *Hind*III sites, whereas the 155-bp product from the *Min* allele contains only one *Hind*III site. *Hind*III digestion of PCR-amplified DNA from *Min*/+ heterozygous tissue results in a 123-bp product from the *Apc*^{+/+} allele and a 144-bp product from the *Apc*^{Min} allele (31). The *Apc*^{+/+}/*Apc*^{Min} ratio was determined by quantitating ³²P-labeled products with ImageQuant software (Molecular Dynamics, Sunnyvale, CA). This assay has been shown to be linear over a wide range of input DNA

quantities (31). However, even with stringent techniques to exclude normal cell contamination from tumor samples, some *Apc*⁺ signal is almost always seen in tumor samples (31). Numerous comparisons of normal and intestinal tumor samples have allowed us to conclude that an average *Apc*^{+/+}/*Apc*^{Min} ratio of less than or equal to 0.30 is indicative of extensive *Apc*⁺ loss (31). Samples were assayed at least twice, independently. Only samples that gave repeated values within 10% of each other were included in the results.

Analysis of *Apc* Truncating Mutations. Truncating mutations within the *Apc* ORF were identified by a modification of an assay for IVSP described previously (32, 42, 43). Exon 15 of *Apc* was analyzed by producing four overlapping PCR products (segments 2–5) by amplification of DNA obtained from OCT-embedded or freshly frozen tissue samples. With one exception, the PCR primers used for amplification of segments 2–5 were as described previously (32). The sequence of the reverse primer used for segment 3 was 5'-CTGCCTTCTGTAGGAATGGTATCTCG-3', which corresponds to nucleotides 5053–5078 of the mouse *Apc* ORF (30). Each PCR for segments 2–5 was done in a 50 μ l reaction volume with 2–3 μ l of sample DNA and contained 0.36 μ M forward primer, 0.3 mM each dNTP, 10 mM Tris-HCl (pH 9.0 at 25°C), 50 mM KCl, 0.1% Triton X-100, and 2 units of *Taq* polymerase. For segment 2, each PCR contained 1.12 μ M reverse primer and 1.57 mM MgCl₂; for segment 3, each PCR contained 0.82 μ M reverse primer and 3.0 mM MgCl₂; for segment 4, each PCR contained 1.0 μ M reverse primer and 2.5 mM MgCl₂; and for segment 5, each PCR contained 1.0 μ M reverse primer and 3.0 mM MgCl₂. All segment 2–5 PCRs were performed under the following conditions: 95°C for 3 min followed by 35 cycles of 95°C for 30 s, 55°C for 2 min, and 70°C for 3 min, and finally one cycle of 70°C for 5 min. Amplification of exons 1–14 of *Apc* was performed via RT-PCR with RNA obtained from freshly frozen tissue samples. The region of *Apc* covering exons 1–14 was amplified as either one full-length product (segment 1) or two smaller, overlapping products (segments 1A and 1B). RT was performed with 1–5 μ g of total RNA in a 50- μ l reaction with Superscript II reverse transcriptase (Life Technologies, Inc., Gaithersburg, MD), according to the manufacturer's protocol. The *Apc*-specific primer used to prime the RT reaction; 5'-GCCACACAATGGAACTCGG-3', corresponds to nucleotides 2723–2741 of *Apc* (30). Four μ l of each RT reaction were used directly in each 50- μ l PCR. The primers for segment 1 have been described previously (32). The forward primer for segment 1A was the same as that for segment 1. The reverse primer for segment 1A, 5'-CATCTCACAGTCCACCTGC-3', corresponds to nucleotides 1431–1449 of the *Apc* ORF (30). The reverse primer for segment 1B was the same as that for segment 1. The forward primer for segment 1B was 5'-GGATCCTAATACGACTCACTATAGGGAGACCACCATGGGTGAAC-CTGTTGGGAGTGG-3'. The *Apc*-specific portion of this primer (in italics) corresponds to nucleotides 1244–1263 (30). All RT-PCRs contained 1.12 μ M forward primer, 0.38 μ M reverse primer, 0.2 mM each dNTP, 2.7 mM MgCl₂, 10 mM Tris-HCl (pH 9.0 at 25°C), 50 mM KCl, 0.1% Triton X-100, and 3 units of *Taq* polymerase. All RT products were PCR-amplified under the following conditions: 95°C for 3 min, followed by 40 cycles of 95°C for 30s, 60°C for 2 min, and 70°C for 3 min, and finally one step at 70°C for 5 min.

The quality and quantity of all PCR products were assessed by running 5 μ l of each reaction on 1% agarose gels. Products of successful PCR amplifications were extracted with phenol-chloroform and precipitated with ethanol, and 50–100% of each PCR amplicon was used in a 25- μ l coupled *in vitro* transcription-translation reaction following the manufacturer's protocol (Promega Corp., Madison, WI). [³⁵S]Methionine-labeled polypeptides from these reactions were analyzed by 8–14% SDS-PAGE. Gels were fixed, dried, and then exposed to film and/or PhosphorImager screens.

***Apc* Sequencing.** Several of the *Apc* truncations identified by the IVSP assay were further characterized by sequence analysis. Sequencing was performed by cycle sequencing of PCR products with either ³²P-labeled primers and the dsDNA Cycle Sequencing System (Life Technologies, Inc.) or with dye-labeled primers and the Dye Primer Cycle Sequencing System (Perkin-Elmer Corp., Foster City, CA). Cycle sequencing conditions were as described by each manufacturer. In both cases, sequencing products were analyzed by electrophoresis through 6% denaturing polyacrylamide gels. Prior to sequencing, PCR products were purified by either the QIAquick PCR purification method (Qiagen Inc., Chatsworth, CA) or MicroSpin S-400 HR columns (Pharmacia Biotech, Uppsala, Sweden). Internal sequencing primers were designed on the basis of the approximate location of the individual truncations. For dye primer sequencing, M13 tailed primers were used for the PCR such

Table 1 Analysis of *Apc* allelic status in intestinal tumors from ENU-treated *Min/+* mice

The average intestinal tumor multiplicity and percentage of tumors with *Apc*⁺ retention for a given ENU treatment age are shown. B6 *Min/+* mice were treated with a single i.p. injection of ENU at 5–35 days of age and then sacrificed approximately 65 days after treatment. Untreated B6 *Min/+* mice were sacrificed at an age corresponding to the final age of the treated mice (i.e. 70–100 days).

Age at ENU treatment, days	Average intestinal tumor multiplicity (\pm SD) ^a	Percentage of total tumors with <i>Apc</i> ⁺ retention ^b	Estimated proportion of ENU-induced tumors with <i>Apc</i> ⁺ retention ^c	<i>Apc</i> ⁺ / <i>Apc</i> ^{Min} ratio ^d	
				Tumors that retained <i>Apc</i> ⁺ ^e	Tumors that lost <i>Apc</i> ⁺ ^f
5–9	104.1 \pm 25.1	40 (8/20)	42/75 (56%)	0.79 \pm 0.20	0.15 \pm 0.06
10–14	116.2 \pm 33.0	50 (13/26)	58/87 (67%)	0.55 \pm 0.14	0.09 \pm 0.06
15–19	74.1 \pm 17.8	59 (16/27)	44/45 (98%)	0.58 \pm 0.15	0.17 \pm 0.04
20–25	54.3 \pm 18.7	23 (7/30)	13/25 (52%)	0.43 \pm 0.15	0.12 \pm 0.07
30–35	41.4 \pm 9.0	29 (9/31)	12/12 (100%)	0.57 \pm 0.34	0.17 \pm 0.07
Untreated	29.2 \pm 9.4	0 (0/12)			

^a See Ref. 36.

^b *Apc*⁺ retention is based on a *Apc*⁺/*Apc*^{Min} ratio greater than 0.30.

^c Values were calculated based on the predicted number of ENU-induced tumors (column 2) and the observed percentage of *Apc*⁺ marker retention (column 3) for each age group.

^d Mean \pm SD of the ratio for the 12 tumor samples collected from untreated B6 *Min/+* mice is 0.17 \pm 0.07. Mean \pm SD of the ratio for 54 normal intestinal tissue samples collected from B6 *Min/+* mice treated with ENU at 5–35 days of age is 0.70 \pm 0.15.

^e Means and SDs of the *Apc*⁺/*Apc*^{Min} ratio for the population of tumors that retained *Apc*⁺ for each age group.

^f Means and SDs of the ratio for the population of tumors that lost *Apc*⁺ for each group.

that dye-labeled-21M13 or M13Rev primers could be used in the cycle sequencing reactions.

Ras Mutational Analyses. Codons 12, 13, and 61 of both K- and H-*ras* were examined for mutations via dye primer cycle sequencing of PCR products, as described above. The forward and reverse primers used for PCR amplifications were as follows: K-*ras* exon 1 (covering codons 12 and 13), 5'-TTATTGTAAAG-GCCTGCTGAA-3' and 5'-GCAGCGTTACCTCTATCGTA-3'; K-*ras* exon 2 (covering codon 61), 5'-TTCTCAGGACTCCTACAGGA-3' and 5'-ACCCACCTATAATGGTGAAT-3'; H-*ras* exon 1, 5'-GACAGAATACAAGCTTGTG-3' and 5'-AGTGGGATCATACTCGTCC-3'; H-*ras* exon 2, 5'-AACAGGTGGT-CATTGATGGG-3' and 5'-ATGGATGCTCCTCGAAGGACTTGG-3'. In each case, one of the forward or reverse primers was M13 tailed for subsequent cycle sequencing. For K-*ras* PCR amplification, each reaction contained 0.25 μ M each primer, 0.25 mM each dNTP, 2.5 mM MgCl₂, 10 mM Tris-HCl (pH 9.0 at 25°C), 50 mM KCl, 0.1% Triton X-100, and 0.75 unit of *Taq* polymerase. Each PCR was amplified under the following conditions: 94°C for 3 min, followed by 30 cycles of 94°C for 30s, 40°C for 2 min, and 72°C for 2 min, and finally one step at 72°C for 5 min. For H-*ras* amplifications, each reaction contained 0.38 μ M each primer, 0.25 mM each dNTP, 10 mM Tris-HCl (pH 9.0 at 25°C), 50 mM KCl, 0.1% Triton X-100, 0.75 unit of *Taq* polymerase, and either 1.5 mM (exon 1) or 0.8 mM (exon 2) MgCl₂. The amplification profile for H-*ras* was the same as for K-*ras* except that the annealing temperature was 45°C instead of 40°C. In addition, the hot start technique was used for K- and H-*ras* amplifications (44).

RESULTS

Somatic *Apc*⁺ Allele Loss in Intestinal Tumors from ENU-treated B6 *Min/+* Mice. We examined intestinal tumors from ENU-treated B6 *Min/+* mice for *Apc*⁺ loss using a quantitative PCR assay (see "Materials and Methods" and Ref. 31). This assay tests for the presence or absence of nucleotides 2524–2679 from both the *Apc*^{Min} and *Apc*⁺ alleles. For these experiments, DNA was prepared from scraped sections of formalin-fixed intestinal tissue. This method allows for relatively stringent exclusion of normal intestinal cells from the tumor DNA samples (31).

A summary of the analysis of *Apc* allelic status in intestinal tumors from untreated and ENU-treated B6 *Min/+* mice is presented in Table 1. The average number of ENU-induced intestinal tumors was calculated by subtracting the average tumor multiplicity for untreated mice (29.2) from the average total tumor multiplicity for each treatment group. Under the assumption that all spontaneously arising tumors lose *Apc*⁺ (see Ref. 31), the estimated proportion of ENU-induced tumors that retained the *Apc*⁺ marker was calculated by dividing the predicted total number of tumors showing *Apc*⁺ retention by the number of putatively ENU-induced tumors (Table 1).

Some of the tumors from B6 *Min/+* mice treated with ENU at all five ages retained the *Apc*⁺ allelic marker (Table 1). For mice treated at either 15–19 or 30–35 days of age, nearly 100% of the ENU-

induced tumors were predicted to retain *Apc*⁺. However, for mice treated at the other three ages, some putatively ENU-induced tumors showed *Apc*⁺ retention, and others showed *Apc*⁺ loss (Table 1).

***Apc* Truncation Mutations in Intestinal Tumors from ENU-treated B6 *Min/+* Mice.** The results from the analysis of *Apc* allelic status for ENU-induced tumors indicated that at least some of these tumors can form without complete deletion of the *Apc*⁺ allele. To identify more subtle *Apc* mutations, intestinal tumors from ENU-treated B6 *Min/+* mice were examined for somatic *Apc* mutations by use of a IVSP assay described previously that specifically detects *Apc* truncation mutations (32, 42, 43). Tumors were first screened for *Apc* allelic loss with the quantitative PCR assay, and tumors that retained the *Apc*⁺ marker (*Apc*⁺/*Apc*^{Min} > 0.30) were subsequently screened for *Apc* truncations. Because the *Apc* truncation assay is incompatible with nucleic acid prepared from formalin-fixed tissue, we used frozen tissue samples for these experiments. In one set of experiments, intestinal tumors and normal intestinal epithelial samples were dissected from B6 *Min/+* mice and quickly frozen in OCT compound. Samples were then sectioned, approximately every tenth section was collected for histological analysis, and the rest of the sections were used for DNA preparation.

Sixty-one % (55 of 90) of the tumors collected in this fashion from B6 *Min/+* mice treated with ENU at 8–19 days of age (mean age, 15.2 days) were classified as retaining *Apc*⁺. Twenty-six of these tumors were collected from the small intestine, whereas the other 29 tumors were from the colon. The average (\pm SD) *Apc*⁺/*Apc*^{Min} ratio for the 55 tumors that retained the region of *Apc*⁺ tested was 0.48 \pm 0.11. The average (\pm SD) ratio for the 35 tumors with *Apc*⁺ loss was 0.17 \pm 0.07. The average (\pm SD) ratio for 18 normal intestinal tissue samples collected from these ENU-treated *Min/+* mice was 0.55 \pm 0.10.

It is unclear why the ratio for the normal tissue controls for the OCT-embedded and freshly frozen samples (see below) was lower than observed for formalin-fixed normal tissue controls (Table 1 and Ref. 31). A similar discrepancy has also been observed in other experiments involving fresh versus formalin-fixed intestinal tissue samples (A. R. S., unpublished observations). However, the average *Apc*⁺/*Apc*^{Min} ratio for the tumors classified as showing allelic loss from both the OCT-embedded and freshly frozen samples fell below that for the normal tissue controls by greater than 4 SDs. In contrast, the average ratio for the tumors classified as retaining *Apc*⁺ fell within 1 SD of the average control ratios.

Of the 55 tumors from these ENU-treated mice that retained the *Apc*⁺ allelic marker, 46 were screened by IVSP for truncations in segment 2 of *Apc* (approximately covering codons 680–1230). Ten

truncations were identified in this region (Fig. 1). Seven of these truncations were found in colon tumors, and three occurred in tumors from the small intestine. The simultaneous presence of the truncated polypeptide from the *Min* allele indicates that the novel truncations had occurred in the *Apc*⁺ allele (Fig. 1). For the remaining 36 tumors that did not have truncations in segment 2, 20 were also screened for segment 3 (approximately covering codons 765–1690), and 9 were screened for segments 3 and 4 (approximately covering codons 1550–2270). No truncations were identified in any of these 36 samples.

The specific mutations responsible for 6 of the 10 truncations were identified by sequence analysis of *Apc* (Table 2, samples not marked with an asterisk). All of these mutations were single base pair substitutions that resulted in nonsense mutations (Table 2). For the remaining four samples with truncations, *Apc* sequencing was either not successful or not possible because of limited sample DNA. No somatic *Apc* truncations were observed in control samples obtained from normal intestinal epithelium from ENU-treated *Min*/+ mice or from tumor and normal tissue samples from untreated *Min*/+ mice (data not shown). Analysis of H&E-stained sections revealed no histological differences between intestinal tumors with *Apc*⁺ loss and tumors with *Apc*⁺ retention, either with or without accompanying *Apc* truncation (data not shown).

Primarily owing to difficulties with RT of RNA obtained from OCT-embedded samples, the entire ORF of *Apc* could not be examined for truncations in this set of samples. To examine the entire ORF of *Apc*, a third set of tumor samples was collected. In this experiment, tumor and normal intestinal samples were dissected from B6 *Min*/+ mice, and individual samples were cut in half for separate preparation of DNA and RNA (see "Materials and Methods").

Sixty % (45 of 70) of the tumors collected in this fashion from B6

Table 2 Somatic *Apc* mutations in intestinal tumors from ENU-treated B6 *Min*/+ mice

Sample ^a	Wild-type <i>Apc</i> sequence ^b	Change ^c	Codon
4855	5'-ATGGTTAAAA-3'	T → A (Tyr → stop)	971
5053	5'-GTATCCAGCT-3'	T → A (Tyr → stop)	998
5049	5'-ATTCTGAGAA-3'	T → A (Tyr → stop)	1076
4977*	5'-ACAACAAGAA-3'	C → T (Gln → stop)	1094
5063	5'-AAGAACAACA-3'	C → T (Gln → stop)	1150
4860	5'-CTCACAAAAA-3'	C → G (Ser → stop)	1189
4854	5'-CTCACAAAAA-3'	C → T (Ser → stop)	1190
4978*	5'-CTCACAAAAA-3'	C → T (Ser → stop)	1190
4975*	5'-TCTCAAAGAA-3'	C → G (Ser → stop)	1197

^a All samples are tumors that were dissected from the large intestine of ENU-treated B6 *Min*/+ mice. Samples marked with an asterisk are from freshly frozen tumors. The remaining samples are from OCT-embedded tumors. These tumors were first shown to have retained the *Apc*⁺ allelic marker by quantitative PCR and then were shown to have *Apc* truncations by IVSP assay (see "Materials and Methods").

^b The sequence represents the region of *Apc* sequence that surrounds a given mutation (underlined).

^c Sequencing was performed as described in "Materials and Methods."

Min/+ mice treated with ENU at 10–13 days of age (mean age, 11.7 days) retained the *Apc*⁺ allelic marker. Eleven of these tumors were collected from the small intestine, whereas the other 34 tumors were from the colon. The average (\pm SD) *Apc*⁺/*Apc*^{Min} ratio for the 45 tumors with *Apc*⁺ retention was 0.50 ± 0.12 . The average (\pm SD) ratio for the 30 tumors with *Apc*⁺ loss was 0.12 ± 0.08 . The average (\pm SD) ratio for 28 normal intestinal tissue control samples was 0.52 ± 0.08 .

Fifteen *Apc* truncations were identified from the set of 45 tumors that retained *Apc*⁺. All but one of these truncations occurred in tumors from the large intestine. Thirteen of these 15 truncations were found in segment 2 of *Apc*, whereas the other 2 truncations were located near the end of segment 1 (approximately covering codons 1–850). The mutations responsible for 3 of these 15 truncations were identified by sequence analysis of *Apc* (Table 2, samples marked with an asterisk). All three were single base pair substitutions resulting in nonsense mutations. For the remaining 12 samples with truncations, *Apc* sequencing was either not successful or not possible because of limited sample DNA.

The entire ORF of *Apc* was analyzed by IVSP for 12 of the remaining 30 tumors, and no truncations were found (data not shown). For the other 18 tumors, the entire ORF of *Apc* could not be analyzed by IVSP, primarily owing to difficulty in analysis of segment 1. However, segment 2 was analyzed for all of these 18 tumors with no truncations identified. Furthermore, all of exon 15 (segments 2–5) of *Apc* was examined for 7 of these 18 tumors, again with no truncations observed (data not shown).

All of the 25 truncations that we have identified would terminate *Apc* approximately between amino acids 700 and 1215 (Fig. 2). The nine somatic nonsense mutations that were successfully sequenced lie between codons 971 and 1197 of *Apc*. Three of these nine mutations occurred in a tract of sequence between nucleotides 3564 and 3573 of *Apc* that reads 5' CTCACAAAAA 3'. These three mutations (which occurred at the underlined Cs, with two of the three mutations occurring at the same C) consist of one tumor with a C/G→T/A (Ser→stop, amino acid 1189) at nucleotide 3566 and two separate tumors with C/G→T/A (Gln→stop, amino acid 1190) changes at nucleotide 3568. Furthermore, 9 of the 25 truncated *Apc* products produced bands of very similar size by SDS-PAGE. Although only five of the nine mutations were identified by sequence analysis, the IVSP results suggest that all nine would terminate *Apc* approximately between amino acids 1100 and 1200.

Analysis of Intestinal Tumors from *Min*/+ Mice for *ras* Mutations. The status of the *ras* oncogene in intestinal tumors from *Min*/+ mice was determined by sequence analysis. Nine intestinal tumors

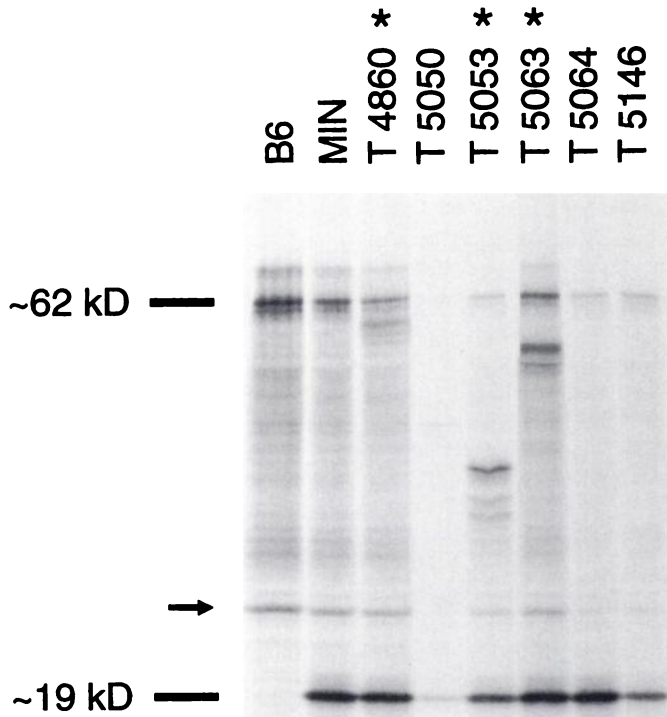


Fig. 1. IVSP assay of segment 2 of *Apc* for truncation mutations in tumors from ENU-treated B6 *Min*/+ mice. Lanes B6 and MIN, analysis of control genomic DNA from B6 *Apc*^{+/+} and B6 *Apc*^{Min/+} mice, respectively. The other six lanes represent analysis of intestinal tumors from ENU-treated B6 *Apc*^{Min/+} mice. The full-length product from segment 2 of *Apc* (approximately covering codons 680–1230) is approximately 62,000 (*M_r*). The polypeptide product resulting from truncation at the *Min* mutation (codon 850 of *Apc*) is approximately 19,000 (*M_r*). Arrow, a nonspecific background band. Lanes marked with an asterisk display truncated products (see Table 2).

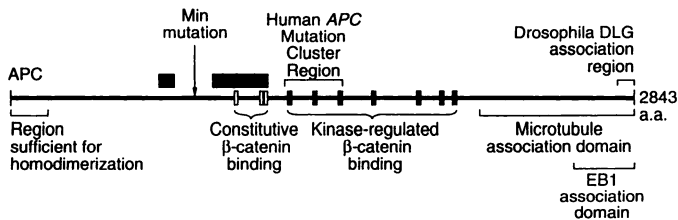


Fig. 2. Location of somatic *Apc* truncation mutations found in intestinal tumors from ENU-treated B6 *Min*⁺ mice relative to binding domains identified in human APC. The *Min* mutation is located at codon 850 of *Apc* (30). The locations of potential APC functional domains are indicated. The amino acids of APC corresponding to each domain are as follows: APC homodimerization, 1–171 (15, 16); constitutive β -catenin binding, 1020–1169 (19, 21); kinase-regulated β -catenin binding, 1342–2075 (20); microtubule association domain, 2143–2843 (17, 18); EB1 association domain, 2560–2843 (61); discs large gene association domain, 2771–2843 (62). The human APC MCR covers codons 1286–1513. ■, approximate regions where truncation mutations were found in intestinal tumors from ENU-treated B6 *Min*⁺ mice. All of the truncations identified occurred proximal to the human APC MCR. Polypeptides produced from these mutant alleles would retain the homodimerization domain and, in some cases, at least part of the constitutive β -catenin-binding domain.

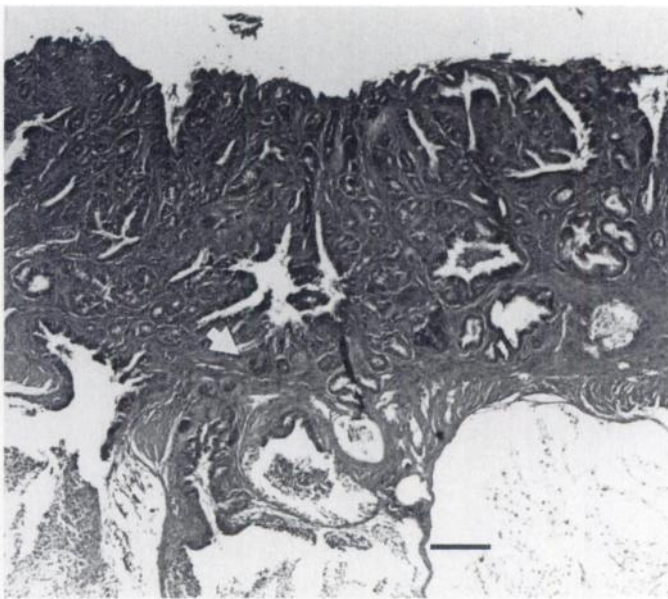


Fig. 3. Photograph of an H&E-stained section of a dysplastic small intestinal adenoma from an untreated (AKR \times B6) F₁ *Min*⁺ mouse. This tumor has become locally invasive (arrow) and contains regions of carcinoma *in situ* (not visible at this magnification). This tumor had lost the *Apc*⁺ allele (*Apc*⁺/*Apc*^{Min} = 0.13) but was wild type at codons 12, 13, and 61 for both K- and H-*ras*. Bar, 200 μ m.

from five untreated (AKR \times B6)F₁ *Min*⁺ mice were analyzed for mutations in codons 12, 13, and 61 of K- and H-*ras*. We have reported previously that on some genetic backgrounds, *Min*⁺ mice can live longer and develop more advanced intestinal tumors (45). The average age of the five F₁ mice used in this experiment was 297 \pm 16 days. The nine tumors examined for *ras* mutations had all lost the *Apc*⁺ allele (average *Apc*⁺/*Apc*^{Min} = 0.20 \pm 0.06). All of the tumors examined were dysplastic adenomas. Two of these tumors were locally invasive and contained regions of carcinoma *in situ* (Fig. 3). Adenomas of this histological grade are the most advanced type of intestinal tumor we observe in *Min*⁺ mice and were thus chosen for our initial examination of *ras* status. We hypothesized that if *ras* activation is important in tumor formation and/or early progression, these relatively advanced tumors would be the most likely class of tumors to contain *ras* mutations.

A summary of the *ras* mutational analyses is presented in Table 3. No *ras* mutations were found in codons 12, 13, or 61 for K-*ras* or for codon 61 of H-*ras* for any of the nine tumors. In addition, no codon

12 or 13 H-*ras* mutations were found in two of the nine tumors (Table 3). The sequence of H-*ras* codons 12 and 13 in the remaining seven tumors could not be unambiguously determined owing to high background signal. Control samples from normal intestinal tissue from these (AKR \times B6)F₁*Min*⁺ mice exhibited wild-type sequence for codons 12, 13, and 61 for both K- and H-*ras* (data not shown). We also examined the status of K-*ras* in 10 of the 12 intestinal tumors from ENU-treated B6 *Min*⁺ that retained the *Apc*⁺ allelic marker and that did not contain truncations in any part of the *Apc* ORF, as tested by IVSP. The other two tumors could not be tested due to limited sample DNA. No codon 12, 13, or 61 K-*ras* activating mutations were identified in any of these 10 tumors (data not shown). These results indicate the mutational activation of K- or H-*ras* is not a common event in the formation of intestinal adenomas in *Min*⁺ mice or their precarcinoma progression.

DISCUSSION

Spontaneously arising intestinal tumors in B6 *Min*⁺ mice lose the wild-type allele of *Apc*, most likely through a mechanism involving whole chromosome loss (31, 32). The intestinal tumor multiplicity of *Min*⁺ mice can be dramatically increased by somatic mutagenesis with the direct-acting alkylating agent ENU (36). We have taken advantage of this mutagenesis result to perform a detailed investigation of the somatic mutational mechanisms involved in intestinal tumor formation in *Min* mice.

Somatic ENU treatment of B6 *Min*⁺ mice at 5–35 days of age gave rise to a population of tumors that retained the *Apc*⁺ allelic marker tested by quantitative PCR assay (Table 1). For mice treated at either 15–19 or 30–35 days of age, nearly all ENU-induced tumors were predicted to retain *Apc*⁺. Treatment at the other ages examined resulted in a mixed population of ENU-induced tumors in which some had lost the *Apc*⁺ allele and others had not (Table 1). We determined that at least 25 of the 100 tumors with *Apc*⁺ retention had acquired somatic *Apc* truncation mutations. All of these truncations occurred approximately between codons 700 and 1215 of *Apc*. The nine nonsense mutations we identified by sequence analysis were located between codons 971 and 1197. Four of these mutations occurred between codons 1189 and 1197 with a C \rightarrow T transition at codon 1190 found in two separate tumors (Table 2). Only 4 of the 25 truncations identified were in tumors from the small intestine. This may be owing to the fact that overall, more colon tumors were screened for mutations and/or that it may be more difficult to detect truncations in tumors of the small intestine, where there is an increased likelihood of introducing normal tissue contamination during sample collection.

Each truncated *Apc* allele found in tumors from ENU-treated mice would encode a product lacking several potential *Apc* functional

Table 3 Summary of *ras* mutational analyses from (AKR \times B6) F₁ *Min*⁺ mice

The dysplastic adenomas from these mice represent the most advanced type of intestinal tumor we observe in *Min*⁺ mice. The status of the *ras* oncogene was examined by sequence analysis (see "Materials and Methods").

Tumor sample	Region of <i>ras</i> analyzed		
	K- <i>ras</i> 12/13/61	H- <i>ras</i> 12/13	H- <i>ras</i> 61
D3543	+ ^a	+	+
D3557	+	ND ^b	+
D3559	+	ND	+
D3839	+	ND	+
D3845	+	ND	+
D3847	+	+	+
D3851	+	ND	+
D4014	+	ND	+
D4015	+	ND	+

^a +, identification of wild-type sequence at the indicated codons (12, 13, or 61) for either K- or H-*ras*. No *ras* mutations were identified in any of the tumors examined.

^b ND, not determined.

domains (Fig. 2). In addition to the binding domains contained in the COOH-terminal 700 amino acids of *Apc*, the kinase-regulated β -catenin-binding domain would also be absent from the products of each of these mutant alleles. However, of the nine alleles in which the specific mutation was identified by sequencing, only two would be missing all three of the 15 amino acid repeats that comprise the constitutive β -catenin-binding domain. All of the truncations would also retain the putative *Apc* homodimerization domain. We do not know whether the binding domains in the products from these truncated alleles are functional, or whether these mutant alleles are expressed *in vivo*. However, an analysis of human cell lines with known *APC* mutations suggested that *APC* polypeptides produced by truncation mutation beyond codon 715 are often stably expressed (46).

Approximately 95% of somatic *APC* mutations in FAP tumors occur in the MCR between codons 1286 and 1513 (5–7). In contrast, about 77% of somatic mutations in sporadic tumors are located in this region (4, 5). It has been proposed that the higher incidence of somatic *APC* mutations in the MCR in FAP tumors relative to sporadic tumors is due to the fact that germ-line *APC* mutations are broadly distributed over the first half of the gene (4). This suggestion is based on an hypothesis that tumor formation is induced more efficiently when at least one allele of *APC* is mutated in the MCR (4). All of the truncations we identified in tumors from ENU-treated B6 *Min/+* mice occurred proximal to the human MCR. Since the *Min* mutation is located in codon 850 of *Apc*, all of the tumors with ENU-induced truncations, as well as tumors with complete *Apc*⁺ allele loss, have neither allele of *Apc* mutated in the MCR. The truncated product of the *Apc*^{Min} allele is expressed in both normal intestinal epithelial cells as well as in intestinal tumor cells from B6 *Min/+* mice (47). This truncated polypeptide contains the homodimerization domain but lacks all of the other known binding domains of *Apc* (Fig. 2). Regardless of whether the *Apc*^{Min} allele retains any functional activity, there are two likely explanations for the location of the ENU-induced *Apc* truncations we observed. One possibility is that somatic mutation approximately between codons 700 and 1215 leads to unstable or unexpressed polypeptides. If these polypeptides are unstable or not expressed, these mutant alleles would be functionally equivalent to the *Apc*⁺ loss seen in tumors from untreated mice. This would contrast with the analysis of human *APC* mutations that showed that polypeptide products resulting from truncation after codon 715 are stably expressed (46). If these truncated alleles are expressed, the truncations we observed may indicate that selective removal of both copies of all of the *Apc*-binding domains beyond amino acid 1215 enhances the likelihood for intestinal tumor formation in *Min/+* mice.

Alkylating agents such as ENU are known to modify preferentially particular residues within DNA (48). In addition, the frequency of ENU-induced mutations can be influenced by the sequence surrounding the modified base (49, 50). Transitions involving G/C→A/T or A/T→G/C and transversions involving A/T→T/A appear to be the most prevalent type of ENU-induced mutation in mammalian cells, particularly when the guanine is preceded by a purine (49, 51–54). No definite pattern of mutation was observed in the nine nonsense mutations we identified. Transition and transversion mutations involving C/G→T/A, T/A→A/T, and C/G→G/C were detected (Table 2). Interestingly, six of the nine mutations occurred just prior to an adenine-rich stretch of sequence (Table 2). This type of sequence specificity has not been reported previously for alkylation-induced mutations. However, in a recent study of human intestinal tumors that demonstrated genomic instability owing to DNA replication error (RER), 49% of identified *APC* mutations occurred within poly(A) tracts (12). For our results, it is unclear whether the 3' poly(A) sequence can enhance the ability of preceding nucleotides to be alkylated and/or affect the ability of such alkylated residues to be

repaired. Speculation about the specificity of these ENU-induced mutations needs to be interpreted with caution. In these experiments we could only detect *Apc* mutations that result in *Apc* truncation, thereby introducing an inherent bias in the types of mutations observed. In addition, it is possible that the ability to identify heterozygous mutations unambiguously can be influenced by the surrounding DNA sequence.

Despite the fact that ENU is believed primarily to cause point mutations, some ENU-induced intestinal tumors showed *Apc*⁺ loss (Table 1). Because the *Apc* allele loss assay that we used examines only a 155-bp region of the gene, we cannot discern whether this loss represents internal *Apc* deletion, regional deletion, or whole chromosome loss. There are several possible explanations for the *Apc*⁺ allele loss observed in ENU-induced tumors. One hypothesis is that this allele loss results from global ethylation damage caused by ENU. Such damage may lead to higher rates of mitotic nondisjunction and intestinal tumor formation would subsequently select for the nondisjunction events affecting *Apc*⁺. Another possibility is that ENU induces mutations at another locus (or loci) that lead, in turn, to genomic instability and consequent *Apc*⁺ loss. Finally, it is possible that mutation of another locus (or loci) is also necessary for tumor formation. In this scenario, *Apc*⁺ allele loss may occur before ENU treatment. ENU would therefore not cause allele loss but rather induce mutation at the other locus (or loci) that synergizes with *Apc*^{Min} hemizyosity in tumor formation.

We identified 12 intestinal tumors from ENU-treated B6 *Min/+* mice that retained the region of *Apc*⁺ tested by quantitative PCR assay and were not found to have *Apc* truncation mutations in any part of the *Apc* ORF. One obvious explanation for this result is that some of these tumors may have acquired *Apc* missense mutations. However, only a relatively small number of missense mutations have been reported from extensive examination of *APC*, including sequence analysis of the entire *APC* ORF (5, 6, 8). Another possibility is that the IVSP assay does not detect 100% of *Apc* truncation mutations and/or that these tumors may have acquired somatic mutations that alter the expression of the *Apc* protein or transcript. Detailed analyses of *APC/Apc* expression in normal as well as neoplastic intestinal tissue are clearly needed to address this issue further.

For analyses involving either OCT-embedded or fresh frozen tumors, there is also a concern with interference in the allele loss assay due to normal cell contamination. Indeed, in an analysis of dissected tumors from a control population of untreated B6 *Min/+* mice that were frozen in OCT and processed in the same manner as tumors from ENU-treated *Min/+* mice, 2 of 15 (13%) had an *Apc*^{+/Apc}^{Min} ratio greater than 0.30 (data not shown). Therefore, a small number of dissected tumors from ENU-treated B6 *Min/+* mice are likely to have been incorrectly classified as retaining the wild-type *Apc* allele, on the basis of the quantitative PCR assay.

A final possible explanation for the lack of *Apc* truncations in these 12 tumors is that a multihit tumor formation pathway exists that is independent of a second mutation to the remaining *Apc*⁺ allele in *Min/+* mice. Even though mutation of *APC* is the most frequently observed somatic mutation in human intestinal tumors, no detailed study has found somatic *APC* mutation in 100% of FAP tumors (5, 7). It seems reasonable to consider a mechanism in which mutation of another locus (or loci) in combination with heterozygosity at *APC/Apc* may be sufficient for some cases of intestinal tumor formation. The discovery of multiple potential binding domains within *APC* enhances the plausibility that mutation of an allele of one of these *APC* binding partners, in conjunction with heterozygosity at *APC*, would allow for tumor formation. Such a mechanism contrasts with the one-locus, two-hit model for tumor suppressor gene activity (55, 56). It should be noted that the mathematical model first proposed by Knudson (57) did

not require that the two mutations occur in the two alleles of the same gene.

One possibility for such a two-locus, two-hit model is suggested by a recent finding that *Apc^{Min}* and activated *ras* may cooperate in tumorigenesis (35). These experiments were made possible by the creation of an SV40 large T conditionally immortalized cell line from the normal intestinal epithelium of B6 *Min/+* mice (58). Cells from *Min/+* mice that also expressed an exogenous copy of activated H-*ras* were found to be capable of forming tumors in nude mice within 17 days of injection (35). Cells from *Apc⁺/Apc⁺* mice that expressed the same activated H-*ras* allele did not form tumors in nude mice until 90 days after injection. Intriguingly, one of the tumors arising from the *Min*-specific cell line retained the region of *Apc⁺* tested by this group (35).

We did not find any codon 12, 13, or 61 K-*ras* mutations in 10 of the 12 intestinal tumors that retained the *Apc⁺* allelic marker and that did not have truncation mutations in the *Apc* ORF. This result argues against a two-locus, two-hit model for intestinal tumor formation involving *Apc^{Min}* and activated *ras*.

Studies of human intestinal tumors of various histological stages indicate that activation of K-*ras* in particular is correlated with the development of larger, more dysplastic adenomas (27, 28). However, a significant percentage of human intestinal cancers do not contain any detectable *ras* mutations (27, 28). To begin to address the role of *ras* in intestinal tumor progression in *Min* mice, we took advantage of the genetic modifier system identified for the *Min* phenotype (37, 45). (AKR × B6)F₁ *Min/+* mice develop fewer tumors and, consequently, live longer than B6 *Min/+* mice (37, 45). Due to this increased lifespan, some intestinal tumors in these F₁ mice become locally invasive and can develop regions of carcinoma *in situ* (45). We used these relatively advanced tumors to examine the role of *ras* in intestinal tumorigenesis in *Min* mice. No codon 12, 13, or 61, K- or H-*ras* mutations were identified in nine dysplastic adenomas from (AKR × B6)F₁ *Min/+* mice, Table 3). Although the number of relatively advanced tumors analyzed here is small, our results indicate that activation of the *ras* oncogene is not an important event in adenoma formation or early progression in *Min/+* mice. Similarly, Smits *et al.*, (59) recently reported a lack of detectable *ras* mutations in intestinal tumors from mice with a targeted mutation at codon 1638 of *Apc*. If *ras* activation is involved in *Min*-dependent tumorigenesis, it may be involved in a different step in progression than has been reported for human intestinal oncogenesis.

Min/+ mice that are also homozygous for a targeted mutation in the *Msh2* DNA mismatch repair gene have been reported to develop approximately 3.5-fold more intestinal tumors than *Min/+* mice that are either wild type or heterozygous at *Msh2* (60). Quantitative PCR analysis of the *Apc* allelic status in tumors from *Min/+ Msh2^{-/-}* mice revealed that the majority of tumors from these mice had not lost the *Apc⁺* allele (60). Unlike our observation of *Apc⁺* loss in ENU-induced tumors, all of the additional tumors caused by *Msh2* deficiency in *Min/+* mice appeared to have retained the *Apc⁺* allelic marker. However, of 15 intestinal tumors from *Min/+ Msh2^{-/-}* that were analyzed immunohistochemically, all were reported to lack staining with an antibody specific for the COOH-terminal 20 amino acids of *Apc* (60). This result suggests that loss of normal *Apc* function is necessary for intestinal tumor formation in *Min/+ Msh2^{-/-}* mice. DNA mismatch repair deficiency caused by *Msh2* mutation does not appear to lead to *Apc⁺* loss by deletion or chromosome loss, as we observed for some ENU-induced tumors from *Min/+* mice. It will be interesting to determine whether tumors from *Min/+ Msh2^{-/-}* mice have acquired somatic *Apc* truncation mutations and, if so, whether these truncations occur in the same region of *Apc* that we have reported here for ENU-induced *Apc* truncations.

We have used somatic ENU mutagenesis to demonstrate that intestinal tumor formation can occur in *Min/+* mice without complete deletion of the wild-type *Apc* allele. Our results indicate that some ENU-induced tumors have lost the *Apc⁺* allele. Analysis of ENU-induced tumors that retained the *Apc⁺* allelic marker revealed that at least 25% of these tumors acquired *Apc* truncation mutations that resemble the type of somatic *APC* mutations often observed in human intestinal tumors. However, the location of these somatic mutations within the *Apc* gene is distinct from the most frequently observed human *APC* mutations. We also found 12 tumors in which no somatic *Apc* mutation could be detected by either of the two techniques. Finally, we have found that activation of the *ras* oncogene does not seem to be a common event in the formation or early progression of adenomas in *Min/+* mice.

ACKNOWLEDGMENTS

Natalie Borenstein, Linda Clipson, Darren Katzung, Melanie McNeley, and Jake Prunuske provided expert technical assistance with these experiments. Histological preparations were performed with the assistance of Harlene Edwards, Paula Frindt, Dana Olson, and Jane Weeks. We thank Dr. Henry Pitot for assessment of histological samples. We also thank Drs. Karen Gould and Ilse Riegel for critical review of the manuscript.

REFERENCES

1. Fearon, E. R., and Vogelstein, B. A genetic model for colorectal tumorigenesis. *Cell*, 61: 759–767, 1990.
2. Groden, J., Thliveris, A., Samowitz, W., Carlson, M., Gelbert, L., Albertsen, H., Joslyn, G., Stevens, J., Spirio, L., Robertson, M., Sargeant, L., Krapcho, K., Wolff, E., Burt, R., Hughes, J. P., Warrington, J., McPherson, J., Wasmuth, J., Le Paslier, D., Adeberrahim, H., Cohen, D., Leppert, M., and White, R. Identification and characterization of the familial adenomatous polyposis coli gene. *Cell*, 66: 589–600, 1991.
3. Kinzler, K. W., Nilbert, M. C., Su, L.-K., Vogelstein, B., Bryan, T. M., Levy, D. B., Smith, K. J., Preisinger, A. C., Hedge, P., McKechnie, D., Finnear, R., Markham, A., Groffen, J., Boguski, M. S., Altschul, S. F., Horii, A., Ando, H., Miyoshi, Y., Miki, Y., Nishisho, I., and Nakamura, Y. Identification of *FAP* locus genes from chromosome 5q21. *Science* (Washington DC), 253: 661–665, 1991.
4. Polakis, P. Mutations in the *APC* gene and their implications for protein structure and function. *Curr. Opin. Genet. Dev.*, 5: 66–71, 1995.
5. Miyaki, M., Konishi, M., Kikuchi-Yanoshita, R., Enomoto, M., Igarai, T., Tanaka, K., Muraoka, M., Takahashi, H., Amada, Y., Fukayama, M., Maeda, Y., Iwama, T., Mishima, Y., Mori, T., and Koike, M. Characteristics of somatic mutation of the adenomatous polyposis coli gene in colorectal tumors. *Cancer Res.*, 54: 3011–3020, 1994.
6. Nagase, H., and Nakamura, Y. Mutations of the *APC* (Adenomatous Polyposis Coli) gene. *Hum. Mutat.*, 2: 425–434, 1993.
7. Miyoshi, Y., Nagase, H., Ando, H., Horii, A., Ichii, S., Nakatsuru, S., Aoki, T., Miki, Y., Mori, T., and Nakamura, Y. Somatic mutations of the *APC* gene in colorectal tumors: mutation cluster region in the *APC* gene. *Hum. Mol. Genet.*, 1: 229–233, 1992.
8. Powell, S. M., Zilz, N., Beazer-Barclay, Y., Bryan, T. M., Hamilton, S. R., Thibodeau, S. N., Vogelstein, B., and Kinzler, K. W. *APC* mutations occur early during colorectal tumorigenesis. *Nature* (Lond.), 359: 235–237, 1992.
9. Boman, B. M., and Levin, B. Familial polyposis. *Hosp. Pract.*, 21(5): 155–165, 1986.
10. Aaltonen, L. A., Peltomäki, P., Leach, F. S., Sistonen, P., Pylkkanen, L., Mecklin, J.-P., Järvinen, H., Powell, S. M., Jen, J., Hamilton, S. R., Petersen, G. M., Kinzler, K. W., Vogelstein, B., and de la Chapelle, A. Clues to the pathogenesis of familial colorectal cancer. *Science* (Washington DC), 260: 812–816, 1993.
11. Fishel, R., Lescoe, M. K., Rao, M. R. S., Copeland, N. G., Jenkins, N. A., Garber, J., Kane, M., and Kolodner, R. The human mutator gene homolog *MSH2* and its association with hereditary nonpolyposis colon cancer. *Cell*, 75: 1027–1038, 1993.
12. Huang, J., Papadopoulos, N., McKinley, A. J., Farrington, S. M., Curtis, L. J., Wylie, A. H., Zheng, S., Willson, J. K. V., Markowitz, S. D., Morin, P., Kinzler, K. W., Vogelstein, B., and Dunlop, M. G. *APC* mutations in colorectal tumors with mismatch repair deficiency. *Proc. Natl. Acad. Sci. USA*, 93: 9049–9054, 1996.
13. Lazar, V., Grandjouan, S., Bognel, C., Couturier, D., Rougier, P., Bellet, D., and Bressac-de Paillerets, B. Accumulation of multiple mutations in tumor suppressor genes during colorectal tumorigenesis in HNPCC patients. *Hum. Mol. Genet.*, 3: 2257–2260, 1994.
14. Leach, F. S., Nicolaidis, N. C., Papadopoulos, N., Liu, B., Jen, J., Parsons, R., Peltomäki, P., Sistonen, P., Aaltonen, L. A., Nyström-Lahti, M., Guan, X.-Y., Zhang, J., Meltzer, P. S., Yu, J.-W., Kao, F.-T., Chen, D. J., Cerosaletti, K. M., Fournier, R. E. K., Todd, S., Lewis, T., Leach, R. J., Naylor, S. L., Weissenbach, J., Mecklin, J.-P., Järvinen, H., Petersen, G. M., Hamilton, S. R., Green, J., Jass, J., Watson, P., Lynch, H. T., Trent, J. M., de la Chapelle, A., Kinzler, K. W., and Vogelstein, B. Mutations of a *mutS* homolog in hereditary nonpolyposis colorectal cancer. *Cell*, 75: 1215–1225, 1993.
15. Joslyn, G., Richardson, D. S., White, R., and Alber, T. Dimer formation by an

- N-terminal coiled-coil in the APC protein. Proc. Natl. Acad. Sci. USA, 90: 11109–11113, 1993.
16. Su, L.-K., Johnson, K. A., Smith, K. J., Hill, D. E., Vogelstein, B., and Kinzler, K. E. Association between wild type and mutant APC gene products. Cancer Res., 53: 2728–2731, 1993.
 17. Munemitsu, S., Souza, B., Müller, O., Albert, I., Rubinfeld, B., and Polakis, P. The APC gene product associates with microtubules *in vivo* and promotes their assembly *in vitro*. Cancer Res., 54: 3676–3681, 1994.
 18. Smith, K. J., Levy, D. B., Maupin, P., Pollard, T. D., Vogelstein, B., and Kinzler, K. W. Wild-type but not mutant APC associates with the microtubule cytoskeleton. Cancer Res., 54: 3672–3675, 1994.
 19. Rubinfeld, B., Souza, B., Albert, I., Müller, O., Chamberlain, S., Masiarz, F. R., Munemitsu, S., and Polakis, P. Association of the APC gene product with β -catenin. Science (Washington DC), 262: 1731–1734, 1993.
 20. Rubinfeld, B., Souza, B., Albert, I., Munemitsu, S., and Polakis, P. The APC protein and E-cadherin form similar but independent complexes with α -catenin, β -catenin, and plakoglobin. J. Biol. Chem., 270: 5549–5555, 1995.
 21. Su, L. K., Vogelstein, B., and Kinzler, K. W. Association of the APC tumor suppressor protein with catenins. Science (Washington DC), 262: 1734–1737, 1993.
 22. Kemler, R. From cadherins to catenins: cytoplasmic protein interactions and regulation of cell adhesion. Trends Genet., 9: 317–321, 1993.
 23. Ozawa, M., and Kemler, R. Molecular organization of the uvomorulin-catenin complex. J. Cell Biol., 116: 989–996, 1992.
 24. Miyoshi, Y., Ando, H., Nagase, H., Nishisho, I., Horii, A., Miki, Y., Mori, T., Utsunomiya, J., Baba, S., Petersen, G., Hamilton, S. R., Kinzler, K. W., Vogelstein, B., and Nakamura, Y. Germ-line mutations of the APC gene in 53 familial adenomatous polyposis patients. Proc. Natl. Acad. Sci. USA, 89: 4452–4456, 1992.
 25. Mandl, M., Paffenholz, R., Friedl, W., Caspari, R., Sengteller, M., and Propping, P. Frequency of common and novel inactivating APC mutations in 202 families with familial adenomatous polyposis. Hum. Mol. Genet., 3: 181–184, 1994.
 26. Gayther, S. A., Wells, D., SenGupta, S. B., Chapman, P., Neale, K., Tsioupra, K., and Delhanty, D. A. Regionally clustered APC mutations are associated with a severe phenotype and occur at high frequency in new mutation cases of adenomatous polyposis coli. Hum. Mol. Genet., 3: 53–56, 1994.
 27. Bos, J. L., Fearon, E. R., Hamilton, S. R., Verlaan-de Vries, M., van Boom, J. H., van der Eb, A. J., and Vogelstein, B. Prevalence of *ras* mutations in human colorectal cancers. Nature (Lond.), 327: 293–297, 1987.
 28. Vogelstein, B., Fearon, E. R., Hamilton, S. R., Kern, S. E., Preisinger, A. C., Leppert, M., Nakamura, Y., White, R., Smits, A. M. M., and Bos, J. L. Genetic alterations during colorectal-tumor development. N. Engl. J. Med., 319: 525–532, 1988.
 29. Moser, A. R., Pitot, H. C., and Dove, W. F. A dominant mutation that predisposes to multiple intestinal neoplasia in the mouse. Science (Washington DC), 247: 322–324, 1990.
 30. Su, L. K., Kinzler, K. W., Vogelstein, B., Preisinger, A. C., Moser, A. R., Luongo, C., Gould, K. A., and Dove, W. F. Multiple intestinal neoplasia caused by a mutation in the murine homolog of the APC gene. Science (Washington DC), 256: 668–670, 1992.
 31. Luongo, C., Moser, A. R., Gledhill, S., and Dove, W. F. Loss of *Apc*⁺ in intestinal adenomas from *Min* mice. Cancer Res., 54: 5947–5952, 1994.
 32. Levy, D. B., Smith, K. J., Beazer-Barclay, Y., Hamilton, S. R., Vogelstein, B., and Kinzler, K. W. Inactivation of both APC alleles in human and mouse tumors. Cancer Res., 54: 5953–5958, 1994.
 33. Luongo, C., and Dove, W. F. Somatic genetic events linked to the *Apc* locus in intestinal adenomas of the *Min* mouse. Genes Chromosomes & Cancer, 17: 194–198, 1996.
 34. Kim, S. H., Roth, K. A., Moser, A. R., and Gordon, J. I. Transgenic mouse models that explore the multistep hypothesis of intestinal neoplasia. J. Cell Biol., 123: 877–893, 1993.
 35. D'Abaco, G. M., Whitehead, R. H., and Burgess, A. W. Synergy between *Apc*^{Min} and an activated *ras* mutation is sufficient to induce colon carcinomas. Mol. Cell Biol., 16: 884–891, 1996.
 36. Shoemaker, A. R., Moser, A. R., and Dove, W. F. *N*-Ethyl-*N*-nitrosourea treatment of multiple intestinal neoplasia (*Min*) mice: age-related effects on the formation of intestinal adenomas, cystic crypts, and epidermoid cysts. Cancer Res., 55: 4479–4485, 1995.
 37. Dietrich, W. F., Lander, E. S., Smith, J. S., Moser, A. R., Gould, K. A., Luongo, C., Borenstein, N., and Dove, W. F. Genetic identification of *Mom-1*, a major modifier locus affecting *Min*-induced intestinal neoplasia in the mouse. Cell, 75: 631–639, 1993.
 38. Moser, A. R., Mattes, E. M., Dove, W. F., Lindstrom, M. J., Haag, J. D., and Gould, M. N. *Apc*^{Min}, a mutation in the murine APC gene, predisposes to mammary carcinomas and focal alveolar hyperplasias. Proc. Natl. Acad. Sci. USA, 90: 8977–8981, 1993.
 39. Shedlovsky, A., Guenet, J.-L., Johnson, L. L., and Dove, W. F. Induction of recessive lethal mutations in the T/1-H-2 region of the mouse genome by a point mutation. Genet. Res., 47: 135–142, 1986.
 40. Goelz, S. E., Hamilton, S. R., and Vogelstein, B. Purification of DNA from formaldehyde fixed and paraffin embedded human tissue. Biochem. Biophys. Res. Commun., 130: 118–126, 1985.
 41. Chomczynski, P., and Sacchi, N. Single-step method of RNA isolation by acid guanidinium thiocyanate-phenol-chloroform extraction. Anal. Biochem., 162: 156–159, 1987.
 42. Powell, S. M., Petersen, G. M., Krush, A. J., Booker, S., Jen, J., Giardiello, F. M., Hamilton, S. R., Vogelstein, B., and Kinzler, K. W. Molecular diagnosis of familial adenomatous polyposis. N. Engl. J. Med., 329: 1982–1987, 1993.
 43. van der Luijt, R., Khan, P. M., Vasen, H., van Leeuwen, C., Tops, C., Roest, P., den Dunnen, J., and Fodde, R. Rapid detection of translation-terminating mutations at the adenomatous polyposis coli (*APC*) gene by direct protein truncation test. Genomics, 20: 1–4, 1994.
 44. Chou, Q., Russell, M., Birch, D. E., Raymond, J., and Bloch, W. Prevention of pre-PCR mis-priming and primer dimerization improves low-copy-number amplifications. Nucleic Acids Res., 20: 1717–1723, 1992.
 45. Moser, A. R., Dove, W. F., Roth, K. A., and Gordon, J. I. The *Min* (multiple intestinal neoplasia) mutation: its effect on gut epithelial cell differentiation and interaction with a modifier system. J. Cell Biol., 116: 1517–1526, 1992.
 46. Smith, K. J., Johnson, K. A., Bryan, T. M., Hill, D. E., Markowitz, S., Willson, J. K. V., Paraskeva, C., Petersen, G. M., Hamilton, S. R., Vogelstein, B., and Kinzler, K. W. The APC gene product in normal and tumor cells. Proc. Natl. Acad. Sci. USA, 90: 2846–2850, 1993.
 47. Shoemaker, A. R., Gould, K. A., Luongo, C., Moser, A. R., and Dove, W. F. Studies of neoplasia in the *Min* mouse. BBA (Rev. on Cancer On-line), 1332(2): F2–F48, 1996.
 48. Friedberg, E. C., Walker, G. C., and Siede, W. DNA Repair and Mutagenesis, p. 32–33. Washington, DC: ASM Press, 1995.
 49. Sendowski, K., and Rajewsky, M. F. DNA sequence dependence of guanine-O⁶ alkylation by the *N*-nitroso carcinogens *N*-methyl and *N*-ethyl-*N*-nitrosourea. Mutat. Res., 250: 153–160, 1991.
 50. Zingg, B. C., Pretsch, W., and Mohrenweiser, H. W. Molecular analysis of four ENU induced triosephosphate isomerase null mutants in *Mus musculus*. Mutat. Res., 328: 163–173, 1995.
 51. Eckert, K. A., Ingle, C. A., Klinedinst, D. K., and Drinkwater, N. R. Molecular analysis of mutations induced in human cells by *N*-ethyl-*N*-nitrosourea. Mol. Carcinog. 1: 50–56, 1988.
 52. Kohler, S. W., Provost, G. S., Fieck, A., Kretz, P. L., Bullock, W. O., Sorge, J. A., Putman, D. L., and Short, J. M. Spectra of spontaneous and mutagen-induced mutations in the *lacI* gene in transgenic mice. Proc. Natl. Acad. Sci. USA, 88: 7958–7962, 1991.
 53. Provost, G. S., and Short, J. M. Characterization of mutations induced by ethylnitrosourea in seminiferous tubule germ cells of transgenic B6C3F1 mice. Proc. Natl. Acad. Sci. USA, 91: 6564–6568, 1994.
 54. Skopek, T. R., Walker, V. E., Cochrane, J. E., Craft, T. R., and Cariello, N. F. Mutational spectrum at the *Hprt* locus in splenic T cells of B6C3F1 mice exposed to *N*-ethyl-*N*-nitrosourea. Proc. Natl. Acad. Sci. USA, 89: 7866–7870, 1992.
 55. Cavanee, W. K., Dryja, T. P., Phillips, R. A., Benedict, W. F., Godbout, R., Gallie, B. L., Murphree, A. L., Strong, L. C., and White, R. L. Expression of recessive alleles by chromosomal mechanisms in retinoblastoma. Nature, (Lond.) 305: 779–784, 1983.
 56. Weinberg, R. A. Oncogenes, antioncogenes, and the molecular bases of multistep carcinogenesis. Cancer Res., 49: 3713–3721, 1989.
 57. Knudson, A. G., Jr. Mutation and cancer: statistical study of retinoblastoma. Proc. Natl. Acad. Sci., USA, 68: 820–823, 1971.
 58. Whitehead, R. H., and Joseph, J. L. Derivation of conditionally immortalized cell lines containing the *Min* mutation from the normal colonic mucosa and other tissues of an "immortomouse"/*Min* hybrid. Epithelial Cell Biol., 3: 119–125, 1994.
 59. Smits, R., Kartheuser, A., Jagmohan-Changur, S., Leblanc, V., Breukel, C., de Vries, A., van Kranen, H., van Krieken, J. H., Williamson, S., Edelmann, W., Kucherlapati, R., Meera Khan, P., and Fodde, R. Loss of *Apc* and the entire chromosome 18 but absence of mutations at the *Ras* and *Tp53* genes in intestinal tumors from *Apc* 1638N, a mouse model for *Apc*-driven carcinogenesis. Carcinogenesis (Lond.), 18: 321–327, 1997.
 60. Reitmaier, A. H., Cai, J. C., Bjerknes, M., Redston, M., Cheng, H., Pind, M. T. L., Hay, K., Mitri, A., Bapat, B. V., Mak, T. W., and Gallinger, S. *Msh2* deficiency contributes to accelerated *Apc*-mediated intestinal tumorigenesis. Cancer Res., 56: 2922–2926, 1996.
 61. Su, L. K., Burrell, M., Hill, D. E., Gyuris, J., Brent, R., Wiltshire, R., Trent, J., Vogelstein, B., and Kinzler, K. W. APC binds to the novel protein EB1. Cancer Res., 55: 2972–2977, 1995.
 62. Matsumine, A., Ogai, A., Senda, T., Okumura, N., Satoh, K., Baeg, G. H., Kawahara, T., Kobayashi, S., Okada, M., Toyoshima, K., and Akiyama, T. Binding of APC to the human homolog of the *Drosophila* discs large tumor suppressor protein. Science (Washington DC), 272: 1020–1023, 1996.